OPEN

Salidroside Regulates Mitochondrial Homeostasis After Polarization of RAW264.7 Macrophages

Xiu-Long Wang, MM, Rui-Xiang Sun, MM, Dong-Xu Li, MM, Zhi-Gang Chen, MM, Xue-Fang Li, MM, Si-Yu Sun, MM, Fei Lin, MD, and Guo-An Zhao, MD

Abstract: Salidroside has anti-inflammatory and antiatherosclerotic effects, and mitochondrial homeostasis imbalance is closely related to cardiovascular disease. The aim of this study was to investigate the effect of salidroside on mitochondrial homeostasis after macrophage polarization and elucidate its possible mechanism against atherosclerosis. RAW264.7 cells were stimulated with 1 $\mu g \cdot mL^{-1}$ Lipopolysaccharide and 50 $ng \cdot mL^{-1}$ IFN-γ establish M1 polarization and were also pretreated with 400 μM salidroside. The relative expression of proinflammatory genes was detected by RT-PCR whereas that of mitochondrial homeostasis–related proteins and nuclear factor kappa-B (NF-κB) was detected by WB. Levels of intracellular reactive oxygen species (ROS), mitochondrial membrane potential, and mass were measured by chemifluorescence whereas that of NF-κB nuclear translocation was detected by immunofluorescence. Compared with the Mφ group, the M1 group demonstrated increased mRNA expression of interleukin-1β , inductible nitric oxide synthase (iNOS), and tumor necrosis factor-α ; increased protein expression of iNOS, NOD-like receptor protein 3, putative kinase 1 , and NF-κB p65 but decreased protein expression of MFN2, Tom20, and PGC-1α; decreased mitochondrial membrane potential and mass; and increased ROS levels and NF-κB p65 nuclear translocation. Salidroside intervention decreased mRNA expression of interleukin-1β and tumor necrosis factor-α compared with the M1 group but did not affect that of iNOS. Furthermore, salidroside intervention prevented the changes in protein expression, mitochondrial membrane potential and mass, ROS levels, and NF-κB p65 nuclear translocation observed in the M1 group. In summary, salidroside ultimately inhibits M1 macrophage polarization and maintains mitochondrial homeostasis after macrophage polarization by increasing mitochondrial membrane potential, decreasing ROS levels, inhibiting NF-κB activation, and in turn regulating the expression of proinflammatory factors and mitochondrial homeostasis–associated proteins.

Key Words: salidroside, mitochondrial homeostasis, macrophage polarization, inflammation, NF-κB signaling

(*J Cardiovasc Pharmacol*™ 2023;81:85–92)

INTRODUCTION

Atherosclerotic cardiovascular disease has become one of the leading causes of death in China, of which macrophage polarization is an important mechanism involved in its development.[1] Mitochondrial homeostasis, referring to the balance between mitochondrial biogenesis and degradation, is mainly regulated by dynamic processes such as mitochondrial division and fusion, cristae remodeling, biogenesis, as well as Ca^{2+} homeostasis, and mitophagy. Disruption of mitochondrial homeostasis is associated with the development of cardiovascular diseases and other conditions.[2,3]

Salidroside (SAL), chemically named 2-(4-hydroxyphenyl) ethyl-β-D-glucoside, is the main bioactive ingredient of the Tibetan medicine derived from *Rhodiola rosea* and has various pharmacological effects such as anti-inflammation, antioxidation, and free radical scavenging.[4,5] Studies have shown that SAL has antiatherosclerotic effects,[6,7] and the mechanisms involved include various pathways such as oxidative stress, inflammation, mitochondrial dysfunction, autophagy, and AMP-activated protein kinase signal transduction.[8–11]

In fact, as a chronic inflammatory disease, a large part of the treatment of atherosclerosis benefits from its inhibition of inflammatory signaling. Liu et al showed that SAL reduced atherosclerotic plaque formation by inhibiting NOD-like receptor protein 3 (NLRP3)-associated endothelial cell pyroptosis.[12] Shi's colleagues found that SAL prevented tumor necrosis factor-α (TNF-α)-induced vascular inflammation by blocking activation of mitogen-activated protein kinase and nuclear factor kappa-B (NF-κB) signaling.[13] Yang et al showed that in addition to protecting endothelial cells from

Received for publication March 14, 2022; accepted August 6, 2022.

From the Life Science Research Center, The First Affiliated Hospital of Xinxiang Medical College, Henan International Joint Laboratory of Cardiovascular Injury and Repair, Henan Heart Mitochondrial Biomedical Engineering Research Center, Xinxiang City, PR China.

Supported by the Key Scientific Research Project Plan of Henan Higher Education Institutions (21A320012), the Science and Technology Research Plan of Henan Provincial Department of Science and Technology (212102310350), the Joint Construction Project of Henan Medical Science and Technology Research Program (LHGJ20190441, LHGJ20190442), the Key R&D and Promotion Project of Henan Province (212102310350), and the Key Scientific Research Project Plan of Henan Higher Education Institutions (21A320012, 22A360017, LHGJ20190468).

The authors report no conflicts of interest.

X.-L. Wang and R.-X. Sun have contributed equally to the manuscript.

Correspondence: Guo-An Zhao, MD, The First Affiliated Hospital of Xinxiang Medical College, Health Road 88, Weihui City, Xinxiang City, Henan Province 453100, China (e-mail: guoanzhao@xxmu.edu.cn) or Fei Lin, MD, Research Center for Biological Science, The First Affiliated Hospital of Xinxiang Medical College, Health Road 88, Weihui City, Xinxiang City, Henan Province 453100, China (e-mail: linfeixixi@aliyun.com).

oxidative stress injury, SAL attenuated endothelial cell senescence by reducing inflammatory cytokines and increasing sirtuins 3 expression.[14] In addition, SAL has been shown to inhibit M1 polarization in macrophages,[15] although its protective effect on mitochondrial homeostasis in the polarized state remains unclear. Therefore, the aim of this study was to investigate the effect of SAL on mitochondrial homeostasis after macrophage polarization, thus elucidating the potential mechanism of action of SAL against atherosclerosis.

MATERIALS AND METHODS

Materials

Lipopolysaccharide (LPS) was obtained from Absin Bioscience Inc. (Shanghai, China). Recombinant murine interferon-γ (IFN-γ) was obtained from PeproTech (Rocky Hill, NJ). SAL was purchased from MedChemExpress (Monmouth Junction, NJ). Cell counting kit-8 (CCK-8) was obtained from Dojindo (Mashiki, Japan). The JC-1 mitochondrial membrane potential assay kit, MitoTracker Red CMXRos dye, reactive oxygen species (ROS) assay kit, and Nuclear and Cytoplasmic Protein Extraction Kit were purchased from Beyotime (Shanghai, China). TRIzol reagent was purchased from Invitrogen (Carlsbad, CA). The RNA reverse transcription kit and RT-PCR Kit were obtained from TaKaRa Bio (Kusatsu, Japan).

The following antibodies were used in the study: peroxisome proliferator-activated receptor-γ coactivator (PGC-1α) rabbit monoclonal antibody (cat. no. AB3242) from Millipore (Burlington, MA); NLRP3 rabbit monoclonal antibody (cat. no. 15101), mitofusin-2 (MFN2) (D2D10) rabbit monoclonal antibody (cat. No. 9482S) from Cell Signaling Technology (Danvers, MA), and rabbit anti-PTEN induced putative kinase 1 (PINK1) antibody (cat. no. ab23707) from Abcam (Cambridge, United Kingdom); and rabbit anti-Tom20 antibody (cat. no. 11802-1-AP) and NF-κB p65 Monoclonal antibody (Cat No. 66535-1-Ig) from ProteinTech Group (Rosemount, IL); and Alexa Fluor 488 (1:800, Cell Signaling Technology Inc, Beverly, MA).

Methods

Culture of RAW264.7 Cells, Establishment of M1 Polarization Model, and SAL Treatment

Cryopreserved RAW264.7 cells (Beina Chuanglian Biotechnology Co, Ltd, Beijing, China) were rapidly thawed in a 37°C water bath within 60 seconds and centrifuged at 200*g* for 5 minutes. The supernatant was discarded, and the pellet was resuspended in complete medium (high-glucose Dulbecco's modified Eagle medium containing 10% FBS and 1% penicillin streptomycin double antibody). Subsequently, the cells were transferred to a culture dish and cultured in a 5% CO2 incubator at 37°C until reaching 70%–80% confluence. Cells were then stimulated with 1 $\mu g \cdot mL^{-1}$ LPS and 50 $ng \cdot mL^{-1}$ IFN-γ to polarize Mφ into M1 macrophages. RNA was extracted after 24 hours. The experiment was divided into Mφ, M1, and M1+SAL groups. For the M1+SAL group, 2×10^5 cells were seeded into 6-well plates and grown to approximately 70% confluence, incubated with 400 μM SAL for 2 hours, and then polarized to M1 macrophages with 1 $\mu g \cdot mL^{-1}$ LPS and 50 $ng \cdot mL^{-1}$ IFN-γ.

Determination of SAL Cytotoxicity by CCK-8 Assay

Cells (100 μL) were inoculated at 5000 cells/well in a 96-well plate and incubated for 24 hours at 37°C under 5% CO_2. Subsequently, 10 μL of different concentrations of SAL (0, 25, 50, 100, 200, and 400 μM) were added to the wells, and the plate was incubated for 24 hours. An aliquot of CCK-8 reagent (10 μL) was added to each well, the plate was incubated for 1 hour, and the absorbance was measured at 450 nm using a SpectraMax Plus384 microplate reader (Molecular Devices, San Jose, CA).

Determination of IL-1β, iNOS, and TNF-α Gene Expression by RT-PCR

Total RNA was extracted from cells using TRIzol reagent according to the manufacturer's instructions. After reverse transcription, mRNA expression levels of interleukin-1β (IL-1β), inductible nitric oxide synthase (iNOS), and TNF-α were determined using the QuantStudio 6 Flex Real-Time PCR system (Thermo Fisher Scientific, Waltham, MA). The primers were synthesized by Jinmiao Biotechnology Co, Ltd, and their sequences are listed in Table 1. The RT-PCR program was as follows: 95°C for 30 seconds, 40 cycles of 95°C for 5 seconds, 55°C for 30 seconds, and 72°C for 30 seconds. Gene expression levels were normalized to that of the internal reference gene glyceraldehyde-3-phosphate dehydrogenase (GAPDH). The relative expression of each gene was calculated using the $2^{-\triangle\triangle Ct}$ method using the Mφ group as the reference.

Determination of Mitochondrial iNOS, NLRP3, MFN2, PGC-1α, PINK1, and Tom20 Protein Expression by WB

Cells were collected and lysed with RIPA buffer, and the protein concentration was determined using the bicinchoninic acid method. The collected proteins were subjected to SDS-PAGE gel electrophoresis, transferred to membranes and blocked with 5% skimmed milk for 1 hour, and then incubated overnight at 4°C with primary antibodies against iNOS (1:1000), NLRP3 (1:1000), MFN2 (1:1000), PGC-1α (1:500), PINK1 (1:1000), and Tom20 (1:1000). Subsequently, the membranes were washed 3 times every 10 minutes with TBST

TABLE 1. Sequences of the Primers Used for RT-PCR Analysis

Gene	Sequence (5′–3′)
IL-1β	F:TCGCAGCAGCACATCAACAAGAG
	R:TGCTCATGTCCTCATCCTGGAAGG
iNOS	F:AAGAGGAAGGAGTCCA GTAACACAGA
	R:ACGAGCAAAGGCGCAGAA
TNF-α	F:AAGCCCTGGTATGAGCCCATCTAT
	R:ATGATCCCAAAGTAGACCTGCCCA
GAPDH	F:GCCTCGTCTCATAGACAAGATG
	R:CAGTAGACTCCACGACATAC

solution, incubated for 1 hour with diluted secondary antibody GAPDH (1:5000), and then washed 3 times every 10 minutes with TBST. ECL luminescence solution was used to visualize the protein bands, which were analyzed using ImageJ software.

Determination of Cellular ROS Levels by Chemifluorescence

Cells were grown to 50% confluence in 6-well plates, incubated with 400 μM SAL for 2 hours, and then polarized to M1 macrophages with 1 $\mu g \cdot mL^{-1}$ LPS and 50 $ng \cdot mL^{-1}$ IFN-γ. ROS levels were measured after 24 hours using the ROS assay kit according to the manufacturer's instructions. In brief, the cell culture medium was removed, an appropriate volume of diluted DCFH-DA solution was added, and cells were incubated at 37°C for 20 minutes. Cells were washed 3 times with serum-free cell culture medium to fully remove DCFH-DA, and cells were observed under a Ts2 inverted fluorescence microscope (Nikon, Tokyo, Japan).

Determination of Mitochondrial Membrane Potential and Mass by Chemifluorescence

Cells cultivated in 6-well plates were grown to 50% confluence, incubated with 400 μM SAL for 2 hours, and then polarized to M1 macrophages with 1 $\mu g \cdot mL^{-1}$ LPS and 50 $ng \cdot mL^{-1}$ IFN-γ. Mitochondrial membrane potential and mass were measured after 24 hours. The JC-1 assay kit was used to measure mitochondrial membrane potential according to the manufacturer's instructions. In brief, the cell culture medium was removed, cells were washed twice with PBS, and 1 mL cell culture medium plus 1 mL prepared JC-1 working solution were added. Cells were incubated at 37°C for 20 minutes, the supernatant was removed, and cells were washed twice with prepared JC-1 buffer (1x). Subsequently, 2 mL culture medium was added to the cells, which were observed under the Ts2 inverted fluorescence microscope (Nikon).

MitoTracker Red dye was used to measure mitochondrial mass. In brief, the cell culture medium was removed, prepared Mito-Tracker Red CMXRos working solution was added to the cells, followed by Hoechst 33,342 staining solution, and cells were incubated at 37°C for 15–30 minutes. Subsequently, the supernatant was removed and 2 mL culture medium was added to the cells, which were observed under the Ts2 inverted fluorescence microscope (Nikon).

Protein Expression and Nuclear Translocation of NF-κB p65 Were Determined by WB and Immunofluorescence

Nuclear and cytosolic proteins were extracted using a Nuclear and Cytoplasmic Protein Extraction Kit (Beyotime, Shanghai, China) following the manufacturer's instructions. Specific procedures for protein quantification and WB were described previously.

To examine the anti-inflammatory effects of SAL, the nuclear translocation of NF-κB was detected by immunofluorescence staining using a fluorescence microscope (Leica). The macrophages were treated with SAL for 2 hours followed by addition of LPS and IFN-γ for 1 hour. After treatment, the macrophages were fixed with 3.7% paraformaldehyde in PBS for 15 minutes and then were permeabilized with 0.1% Triton X-100 in PBS for 10 minutes followed by blocking with 2%

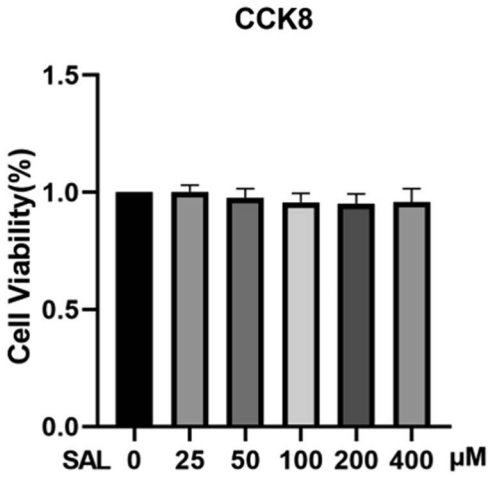

FIGURE 1. The inhibitory effects of different concentrations of SAL (0, 25, 50, 100, 200, and 400 μM) on the viability of RAW264.7 cells, measured using the CCK-8 assay. Values are expressed as the mean ± SD. n = 3 independent experiments.

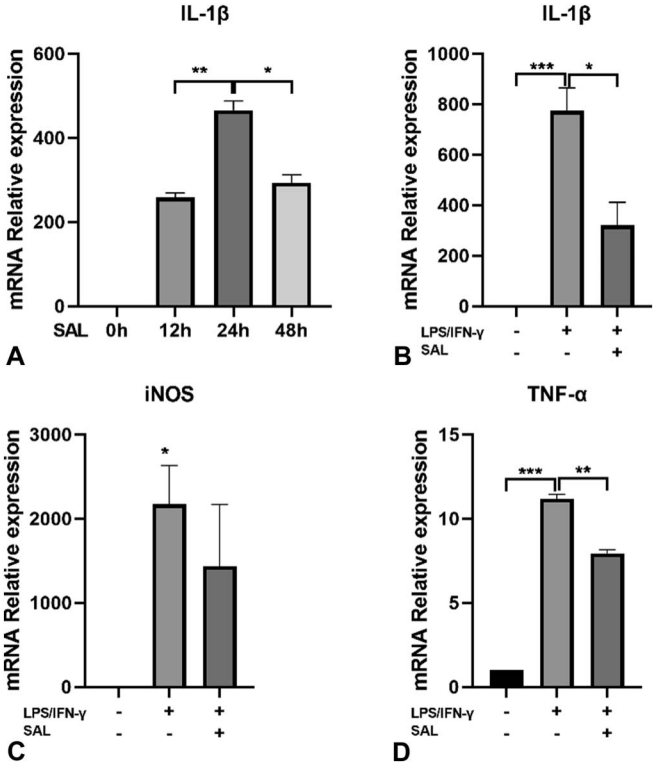

FIGURE 2. The effects of SAL on the expression of proinflammatory genes IL-1β, iNOS, and TNF-α in M1 macrophages, measured using RT-PCR. (A) mRNA expression of IL-1β at 0, 12, 24, and 48 hours after M1 polarization. B–D, mRNA expression of IL-1β, iNOS, and TNF-α after M1 polarization 24 hours with or without SAL. Values are expressed as the mean ± SD. n = 3 independent experiments. *$P < 0.05$, **$P < 0.01$, *** $P < 0.001$.

bovine serum albumin for 30 minutes at room temperature. After washing with PBS, the macrophages were incubated with anti-NF-κB-p65 antibody (1:200, Proteintech for overnight at 4°C). The antimouse IgGk secondary antibody labeled with Alexa Fluor 488 (1:800, Cell Signaling Technology Inc, Beverly, MA) was treated for 1 hour. Nuclei was counterstained with 0.5 μg·mL− 1 DAPI for 10 minutes. After washing with PBS, the stained macrophages were visualized using a fluorescence microscope.

Statistical Analysis

Statistical analysis was performed using GraphPad Prism version 8 software (GraphPad Software, La Jolla, CA). Comparisons between 2 groups were performed using the *t* test, whereas one-way analysis of variance was used to perform comparisons between multiple groups. A *P*-value < 0.05 was considered statistically significant.

RESULTS

Effect of SAL on Proliferative Activity of RAW264.7 Cells

The CCK-8 assay was used to measure the effects of SAL on cell viability. The results indicated that the desired concentration of SAL (400 μM) did not exert cytotoxic effects on RAW264.7 cells within 24 hours, as shown in Figure 1.

Effect of SAL on M1 Macrophages

After RAW264.7 cells were polarized to M1 macrophages, the mRNA expression of IL-1β was measured at 0, 12, 24, and 48 hours. As shown in Figure 2A, IL-1β mRNA expression at 12 and 48 hours was decreased compared with that at 24 hours ($P < 0.01$, $P < 0.05$, respectively). In addition, the mRNA expression of IL-1β, iNOS, and TNF-α in the M1 group was increased compared with that in the Mφ group ($P < 0.001$, $P < 0.05$, $P < 0.001$, respectively), as shown in Figures 2B, D. Meanwhile, the mRNA expression of IL-1β and TNF-α was decreased in the M1+SAL group compared with that in the M1 group ($P < 0.05$, $P < 0.01$, respectively), as shown in Figure 2B, D. Furthermore, iNOS expression did not differ significantly between the M1 and M1+SAL groups, as shown in Figure 2C.

Effect of SAL on Mitochondrial Homeostasis in M1 Macrophages

Measurement of mitochondrial homeostasis–related proteins 24 hours after M1 polarization and SAL intervention

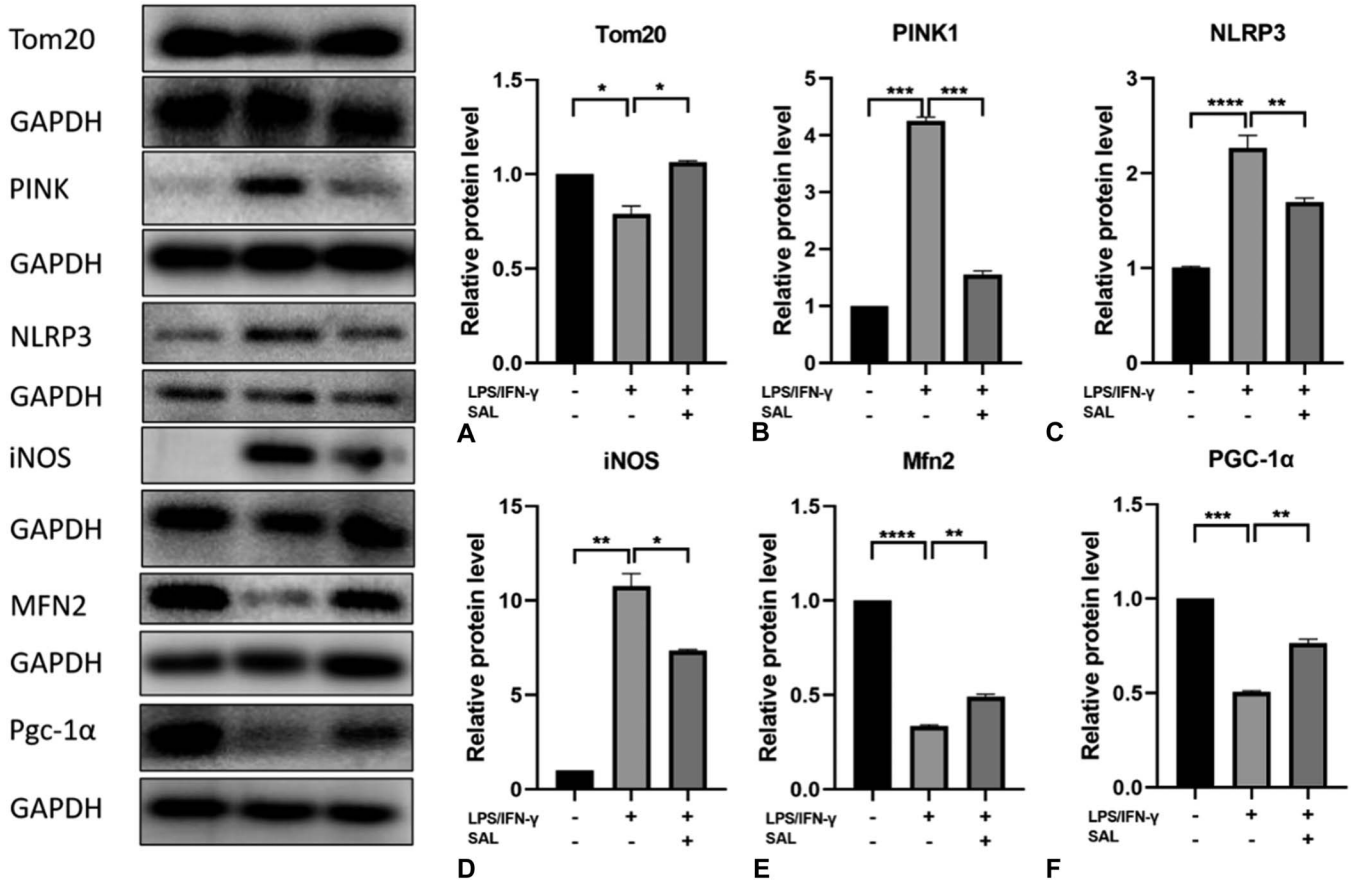

FIGURE 3. The effects of SAL on M1 mitochondrial homeostasis, measured by WB. (A–F) Protein expression of Tom20, PINK1, NLRP3, iNOS, MFN2, and PGC-1α after M1 polarization 24 hours with or without SAL. Values are expressed as the mean ± SD. n = 3 independent experiments. *$P < 0.05$, **$P < 0.01$, *** $P < 0.001$. **** $P < 0.0001$.

revealed that iNOS, NLRP3, and PINK1 protein expression was higher in the M1 group than in the Mφ group ($P < 0.01$, $P < 0.001$, $P < 0.001$, respectively) but lower in the M1+SAL group than in the M1 group ($P < 0.05$, $P < 0.01$, $P < 0.001$, respectively), as shown in Figures 3A, B, and F. Furthermore, the protein expression of MFN2, Tom20, and PGC-1α was lower in the M1 group than in the Mφ group ($P < 0.001$, $P < 0.05$, $P < 0.001$, respectively), but higher in the M1+SAL group than in the M1 group ($P < 0.01$, $P < 0.05$, $P < 0.01$, respectively), as shown in Figures 3C–E.

Effect of SAL on Mitochondrial Membrane Potential and Mass in M1 macrophages

Mitochondrial membrane potential and mass were measured 24 hours after M1 polarization and SAL intervention, revealing that the values of the M1 group were decreased compared with those of the Mφ group ($P < 0.01$, $P < 0.001$, respectively), whereas those of the M1+SAL group were increased compared with those of the M1 group ($P < 0.05$, $P < 0.01$, respectively), as shown in Figure 4.

Effect of SAL on ROS Levels in M1 Macrophages

Detection of intracellular ROS levels 24 hours after M1 polarization and SAL intervention revealed that the ROS levels of the M1 group were higher than those of the Mφ group ($P < 0.001$), whereas those of the M1+SAL group were lower than those of the M1 group ($P < 0.01$), as shown in Figure 5.

Effect of Salidroside on NF-κB p65 Levels and Nuclear Translocation in M1 Macrophages

Detection of NF-κB p65 protein at 24 hours after M1 polarization and SAL intervention showed that NF-κB p65 protein expression was higher in the M1 group than in the Mφ group ($P < 0.0001$) and lower in the M1+SAL group than in the M1 group ($P < 0.0001$). In addition, we detected p65 translocation from the cytoplasm to the nucleus using immunofluorescence and found that nuclear p65 fluorescence staining was enhanced in the M1 group, suggesting increased p65 nuclear translocation, whereas the M1+SAL group attenuated nuclear translocation of NF-κB p65, as shown by attenuation of nuclear p65 fluorescence staining, as shown in Figure 6.

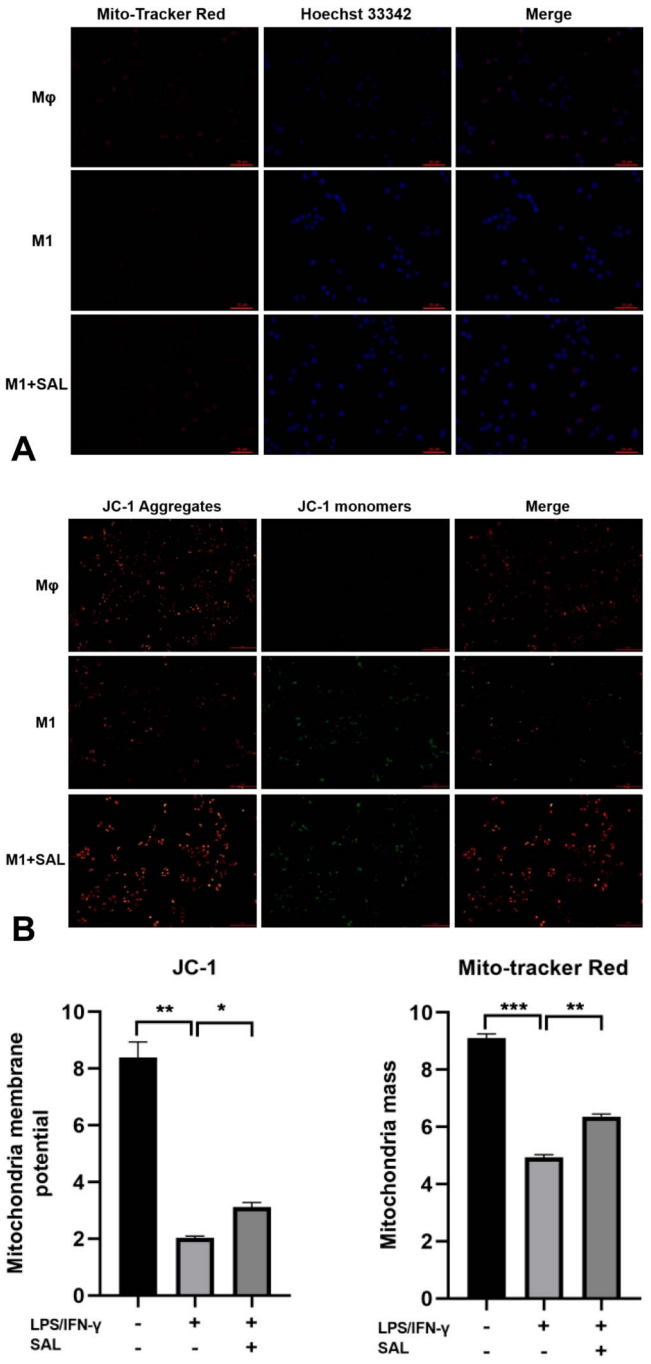

FIGURE 4. The effects of SAL on M1 mitochondrial membrane potential and mass measured by chemifluorescence (× 20). A, Mitochondrial membrane potential after M1 polarization 24 hours with or without SAL. B, Mitochondrial mass after M1 polarization 24 hours with or without SAL. Values are expressed as the mean ± SD. n = 3 independent experiments. *$P < 0.05$, **$P < 0.01$, *** $P < 0.001$.

DISCUSSION

Macrophages are an important part of the body's innate immune system and can be polarized into different subtypes under different microenvironmental conditions. Classically activated (M1) and selectively activated (M2) macrophages play important roles in physiological and pathological processes such as inflammation, defense, repair, and metabolism. Moreover, M1 and M2 macrophages are involved in the development of atherosclerosis and other diseases.[16]

Mitochondria are the main sites of energy metabolism in eukaryotic cells. Mitochondrial homeostasis, the disruption of which is associated with the development of atherosclerosis,[17] is a complex process that includes reducing mitochondrial damage and maintaining mitochondrial stability through proteasome action, ensuring mitochondrial number and morphology through mitochondrial fusion/division, and selectively removing damaged mitochondria by mitophagy.[18,19]

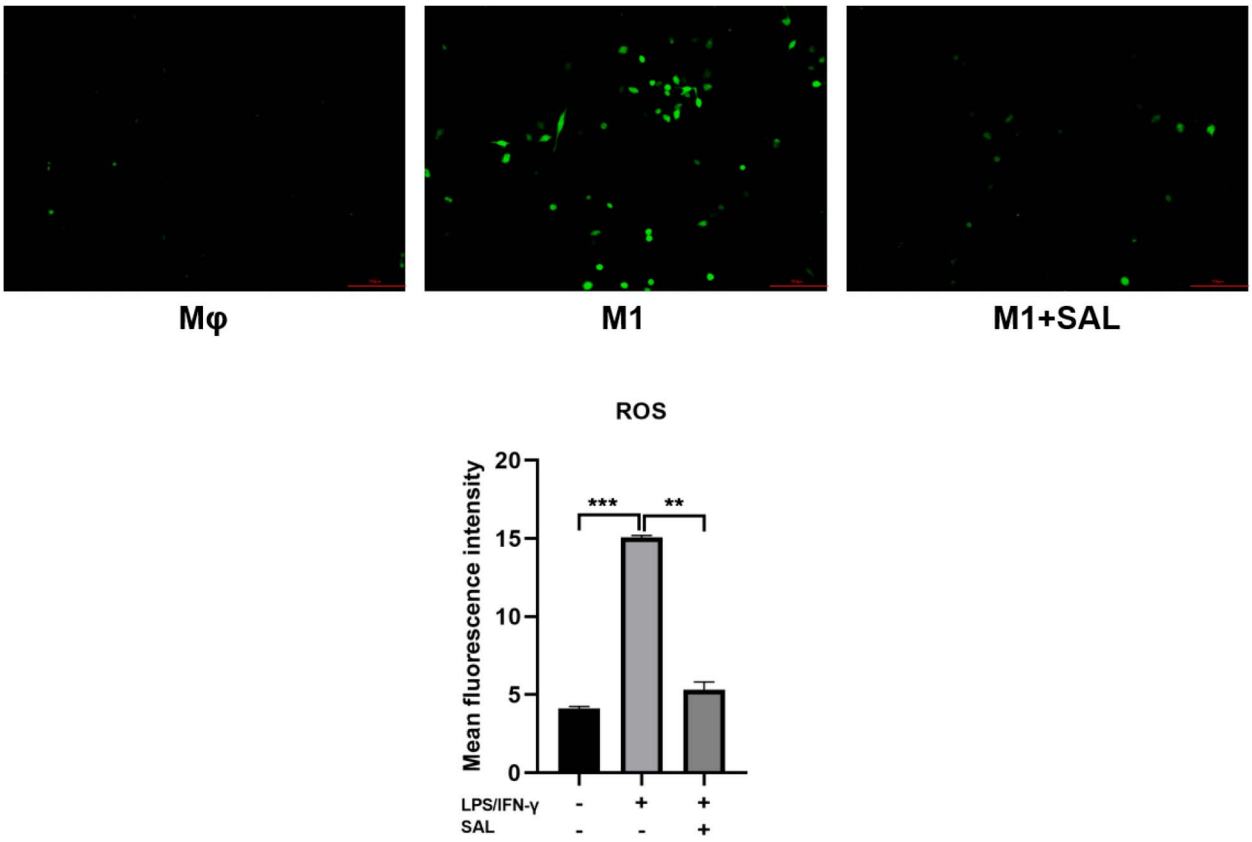

FIGURE 5. Levels of intracellular ROS after M1 polarization 24 hours with or without SAL, measured by chemifluorescence (× 20). Values are expressed as the mean ± SD. n = 3 independent experiments. $^{**}P < 0.01$, $^{***}P < 0.001$.

M1 macrophages have been shown to dominate the progression of atherosclerosis.[20] Indeed, inhibiting the differentiation of intraplaque macrophages to the inflammatory M1 phenotype has been shown to help stabilize vulnerable plaques.[21] LPS, the main component of the outer membrane of Gram-negative bacteria, can stimulate polarization of macrophages to the M1 phenotype, which then secrete a large number of inflammatory factors, such as TNF-α, IL-1β, and iNOS. In the current study, the RT-PCR results indicated that LPS significantly increased the mRNA expression of TNF-α, IL-1β, and iNOS in RAW264.7 cells, which was consistent with literature reports[22–24] and indicated that the macrophage polarization model was successfully constructed. Activation of NLRP3 inflammasomes also plays an important role in the development of atherosclerosis and can mediate M1 macrophage polarization and IL-1β production. As previously reported,[25,26] NLRP3 protein was found to be abundantly expressed in the M1 polarization state in the current study.

Intracellular ROS production mainly occurs in the mitochondria. Excessive ROS production occurs when mitochondria are damaged or antioxidant enzyme synthesis is reduced, which in turn leads to the inactivation of 2 key antiatherosclerotic enzymes: endothelial nitric oxide lyase and prostacyclin lyase.[27] In addition, high ROS levels can cause mitochondrial damage and reduce mitochondrial membrane potential.[28] Mitochondrial damage also disrupts homeostasis, resulting in PINK1 being highly expressed and the initiation of mitophagy.[29] Furthermore, fusion/division becomes abnormal after mitochondrial damage and expression of mitochondrial fusion protein MFN2 is decreased.[30] PGC-1α plays an indispensable role in mitochondria biogenesis and oxidative respiratory function.[31] Under excessive inflammation, PGC-1α synthesis is decreased along with that of mitochondrial outer membrane protein Tom20, which mediates protein transport.[32]

The results of the current study demonstrated that M1 polarization increased intracellular ROS levels, decreased mitochondrial membrane potential, increased PINK1 expression, decreased MFN2 expression, and decreased the synthesis of functional proteins PGC-1α and Tom20. These results were consistent with previous reports, suggesting that mitochondrial homeostasis was disrupted in our M1 polarization state, which may explain why M1 macrophages promote the development of atherosclerosis.

SAL, the main bioactive component of *R. rosea*, has reported therapeutic effects against cardiovascular disease related to its antioxidative and antiapoptotic properties.[33] Previous research by our team demonstrated that SAL inhibited endothelial injury in an atherosclerosis model.[34] In the current study, 400 μM SAL substantially inhibited inflammation by reducing the expression of proinflammatory genes IL-1β, TNF-α, and iNOS in M1 macrophages. Moreover,

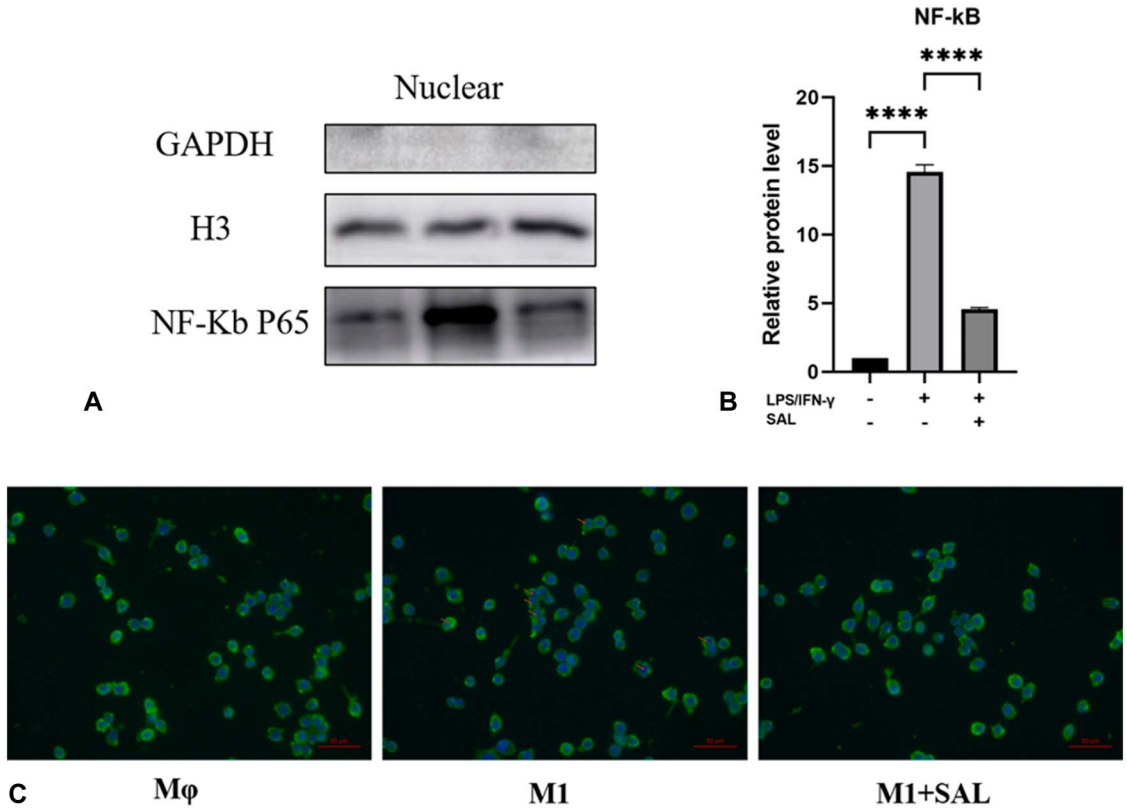

FIGURE 6. Effect of SAL on NF-κB p65 protein expression and nuclear translocation in M1 macrophages. A, B, The expression of NF-κB p65 protein was detected by WB after M1 polarization 24h with or without SAL. C, Changes in p65 nuclear translocation after M1 polarization with or without SAL were detected by immunofluorescence. Values are expressed as the mean ± SD. n = 3 independent experiments. **** $P < 0.0001$.

SAL intervention before M1 polarization decreased ROS levels, increased mitochondrial membrane potential, decreased the expression of autophagy initiator protein PINK1 and NLRP3, and increased the expression of fusion protein MFN2 and functional proteins PGC-1α and Tom20, suggesting that SAL may achieve antiatherosclerotic effects by protecting mitochondrial homeostasis.

As a classical inflammatory signaling pathway, NF-κB pathway is involved in the development of cardiovascular diseases such as atherosclerosis.[35] Mitochondrial monoamine oxidase can impair mitochondrial homeostasis, leading to ROS accumulation and NF-κB activation, thereby enhancing the expression of atherogenic and proinflammatory molecules in endothelial cells.[36] Similarly, oxidative stress in macrophage mitochondria promotes atherosclerosis and NF-κB–mediated inflammation in macrophages.[37] Wu et al point out that new therapies dedicated to correcting mitochondrial dysfunction may represent a promising therapeutic strategy for future treatment and improving atherosclerosis.[38] Therefore, to further investigate, the possible mechanism of the protective effect of SAL on mitochondrial homeostasis after polarization in RAW264.7 macrophages. We examined the expression of NF-κB p65 in M1 polarization as well as changes following SAL intervention. The results showed that M1 polarization increased the expression of NF-κB p65 protein, whereas SAL intervention played the opposite role. Immunofluorescence further verified that p65 nuclear translocation was increased in the M1 group, whereas NF-κB activation was significantly decreased in the SAL group. Thus, SAL may achieve antiatherosclerotic effects by inhibiting NF-κB activation to regulate mitochondrial homeostasis to resist macrophage polarization to M1.

In summary, the results obtained using an M1 macrophage inflammation model of atherosclerosis in the current study demonstrated the protective effect of SAL on mitochondrial homeostasis, thereby providing insight into the mechanism underlying the antiatherosclerosis effects of SAL.

REFERENCES

1. Luo Y, Lu S, Gao Y, et al. Araloside C attenuates atherosclerosis by modulating macrophage polarization via Sirt1-mediated autophagy. *Aging (Albany NY)*. 2020;12:1704–1724.
2. Deshwal S, Fiedler KU, Langer T. Mitochondrial proteases: multifaceted regulators of mitochondrial plasticity. *Annu Rev Biochem.* 2020;89:501–528.
3. Selfridge JE, Lezi E, Lu J, et al. Role of mitochondrial homeostasis and dynamics in Alzheimer's disease. *Neurobiol Dis.* 2013;51:3–12.
4. Yang Z, Huang X, Lai W, et al. Synthesis and identification of a novel derivative of salidroside as a selective, competitive inhibitor of monoamine oxidase B with enhanced neuroprotective properties. *Eur J Med Chem*. 2021;209:112935.
5. Zhang X, Xie L, Long J, et al Salidroside: a review of its recent advances in synthetic pathways and pharmacological properties. *Chem Biol Interact*. 2021;339:109268.

6. Zhang BC, Li WM, Guo R, et al. Salidroside decreases atherosclerotic plaque formation in low-density lipoprotein receptor-deficient mice. *Evid Based Complement Alternat Med.* 2012;2012:607508.
7. Wen SY, Chen YY, Lu JX, et al. Modulation of hepatic lipidome by rhodioloside in high-fat diet fed apolipoprotein E knockout mice. *Phytomedicine*. 2020;69:152690.
8. Bai XL, Deng XL, Wu GJ, et al. Rhodiola and salidroside in the treatment of metabolic disorders. *Mini Rev Med Chem.* 2019;19:1611–1626.
9. Bai X, Jia X, Lu Y, et al. Salidroside-mediated autophagic targeting of active Src and Caveolin-1 suppresses low-density lipoprotein transcytosis across endothelial cells. *Oxid Med Cell Longev*. 2020;2020:9595036.
10. Zhao D, Sun X, Lv S, et al. Salidroside attenuates oxidized low-density lipoprotein-induced endothelial cell injury via promotion of the AMPK/SIRT1 pathway. *Int J Mol Med.* 2019;43:2279–2290.
11. Xing SS, Yang XY, Zheng T, et al. Salidroside improves endothelial function and alleviates atherosclerosis by activating a mitochondria-related AMPK/PI3K/Akt/eNOS pathway. *Vascul Pharmacol.* 2015;72:141–152.
12. Xing SS, Yang J, Li WJ, et al. Salidroside decreases atherosclerosis plaque formation via inhibiting endothelial cell pyroptosis. *Inflammation*. 2020;43:433–440.
13. Li R, Dong Z, Zhuang X, et al. Salidroside prevents tumor necrosis factor-α-induced vascular inflammation by blocking mitogen-activated protein kinase and NF-κB signaling activation. *Exp Ther Med.* 2019;18:4137–4143.
14. Xing SS, Li J, Chen L, et al. Salidroside attenuates endothelial cellular senescence via decreasing the expression of inflammatory cytokines and increasing the expression of SIRT3. *Mech Ageing Dev.* 2018;175:1–6.
15. Liu X, Wen S, Yan F, et al. Salidroside provides neuroprotection by modulating microglial polarization after cerebral ischemia. *J Neuroinflammation*. 2018;15:39.
16. Mouton AJ, Li X, Hall ME, et al. Obesity, hypertension, and cardiac dysfunction: novel roles of immunometabolism in macrophage activation and inflammation. *Circ Res.* 2020;126:789–806.
17. Zheng J, Lu C. Oxidized LDL causes endothelial apoptosis by inhibiting mitochondrial fusion and mitochondria autophagy. *Front Cell Dev Biol*. 2020;8:600950.
18. Zhou H, Ren J, Toan S, et al. Role of mitochondrial quality surveillance in myocardial infarction: from bench to bedside. *Ageing Res Rev.* 2021;66:101250.
19. Li Y, Meng W, Hou Y, et al. Dual role of mitophagy in cardiovascular diseases. *J Cardiovasc Pharmacol*. 2021;78:e30-e39.
20. Liao J, An X, Yang X, et al. Deficiency of LMP10 attenuates diet-induced atherosclerosis by inhibiting macrophage polarization and inflammation in apolipoprotein E deficient mice. *Front Cell Dev Biol*. 2020;8:592048.
21. Ding S, Lin N, Sheng X, et al. Melatonin stabilizes rupture-prone vulnerable plaques via regulating macrophage polarization in a nuclear circadian receptor RORα-dependent manner. *J Pineal Res*. 2019;67:e12581.
22. Li M, Dong L, Du H, et al. Potential mechanisms underlying the protective effects of Tricholoma matsutake singer peptides against LPS-induced inflammation in RAW264.7 macrophages. *Food Chem.* 2021;353:129452.
23. Lin X, Zhang J, Fan D, et al. Frutescone O from Baeckea frutescens blocked TLR4-mediated Myd88/NF-κB and MAPK signaling pathways in LPS induced RAW264.7 macrophages. *Front Pharmacol.* 2021;12:643188.
24. Jiang T, Zhou J, Liu W, et al. The anti-inflammatory potential of protein-bound anthocyanin compounds from purple sweet potato in LPS-induced RAW264.7 macrophages. *Food Res Int.* 2020;137:109647.
25. Abderrazak A, Syrovets T, Couchie D, et al. NLRP3 inflammasome: from a danger signal sensor to a regulatory node of oxidative stress and inflammatory diseases. *Redox Biol.* 2015;4:296–307.
26. Zhang J, Liu X, Wan C, et al. NLRP3 inflammasome mediates M1 macrophage polarization and IL-1β production in inflammatory root resorption. *J Clin Periodontol.* 2020;47:451–460.
27. Giacco F, Brownlee M. Oxidative stress and diabetic complications. *Circ Res.* 2010;107:1058–1070.
28. Zhao M, Wang Y, Li L, et al. Mitochondrial ROS promote mitochondrial dysfunction and inflammation in ischemic acute kidney injury by disrupting TFAM-mediated mtDNA maintenance. *Theranostics*. 2021;11:1845–1863.
29. McLelland GL, Soubannier V, Chen CX, et al. Parkin and PINK1 function in a vesicular trafficking pathway regulating mitochondrial quality control. *EMBO J.* 2014;33:282–295.
30. Luo N, Yue F, Jia Z, et al. Reduced electron transport chain complex I protein abundance and function in Mfn2-deficient myogenic progenitors lead to oxidative stress and mitochondria swelling. *FASEB J.* 2021;35:e21426.
31. Xu W, Yan J, Ocak U, et al. Melanocortin 1 receptor attenuates early brain injury following subarachnoid hemorrhage by controlling mitochondrial metabolism via AMPK/SIRT1/PGC-1α pathway in rats. *Theranostics*. 2021;11:522–539.
32. Wu M, Lu G, Lao YZ, et al. Garciesculenxanthone B induces PINK1-Parkin-mediated mitophagy and prevents ischemia-reperfusion brain injury in mice. *Acta Pharmacol Sin*. 2021;42:199–208.
33. Sun S, Tuo Q, Li D, et al. Antioxidant effects of salidroside in the cardiovascular system. *Evid Based Complement Alternat Med.* 2020;2020:9568647.
34. Zhang Y, Lin F, Yan Z, et al. Salidroside downregulates microRNA-133a and inhibits endothelial cell apoptosis induced by oxidized low-density lipoprotein. *Int J Mol Med.* 2020;46:1433–1442.
35. Cheng W, Cui C, Liu G, et al. NF-κB, A potential therapeutic target in cardiovascular diseases. *Cardiovasc Drugs Ther.* 2022 [Epub ahead of Print].
36. Li Z, Li Q, Wang L, et al. Targeting mitochondria-inflammation circle by renal denervation reduces atheroprone endothelial phenotypes and atherosclerosis. *Redox Biol.* 2021;47:102156.
37. Wang Y, Wang GZ, Rabinovitch PS, et al. Macrophage mitochondrial oxidative stress promotes atherosclerosis and nuclear factor-κB-mediated inflammation in macrophages. *Circ Res.* 2014;114:421–433.
38. Li D, Yang S, Xing Y, et al. Novel insights and current evidence for mechanisms of atherosclerosis: mitochondrial dynamics as a potential therapeutic target. *Front Cel Dev Biol*. 2021;9:673839.